Brain Topogr
DOI 10.1007/s10548-015-0458-y

ORIGINAL PAPER

EEG Correlates of Relative Motion Encoding

Evelina Thunell[1] · Gijs Plomp[1,2] · Haluk Ögmen[3] · Michael H. Herzog[1]

Received: 16 July 2015 / Accepted: 19 October 2015

Abstract A large portion of the visual cortex is organized retinotopically, but perception is usually *non-retinotopic*. For example, a reflector on the spoke of a bicycle wheel appears to move on a circular or prolate cycloidal orbit as the bicycle moves forward, while in fact it traces out a curtate cycloidal trajectory. The moving bicycle serves as a non-retinotopic reference system to which the motion of the reflector is anchored. To study the neural correlates of non-retinotopic motion processing, we used the Ternus–Pikler display, where retinotopic processing in a stationary reference system is contrasted against non-retinotopic processing in a moving one. Using high-density EEG, we found similar brain responses for both retinotopic and non-retinotopic rotational apparent motion from the earliest evoked peak (around 120 ms) and throughout the rest of the visual processing, but only minor correlates of the motion of the reference system itself (mainly around 100–120 ms). We suggest that the visual system efficiently discounts the motion of the reference system from early on, allowing a largely reference system independent encoding of the motion of object parts.

Keywords Apparent motion · Electroencephalography (EEG) · Non-retinotopic processing · Ternus–Pikler display

Electronic supplementary material The online version of this article (doi:10.1007/s10548-015-0458-y) contains supplementary material, which is available to authorized users.

✉ Evelina Thunell
evelina.thunell@cerco.ups-tlse.fr

[1] Laboratory of Psychophysics, Brain Mind Institute, École Polytechnique Fédérale de Lausanne (EPFL), Station 19, 1015 Lausanne, Switzerland

[2] Functional Brain Mapping Lab, Department of Fundamental Neuroscience, University of Geneva, 24 Rue du Général-Dufour, 1211 Geneva 4, Switzerland

[3] Department of Electrical and Computer Engineering, Center for Neuro-Engineering and Cognitive Science, University of Houston, N 308 Engineering Building 1, Houston, TX 77204-4005, USA

Introduction

Neighboring points in the visual field are mapped onto neighboring photoreceptors in the retina, and this retinotopic encoding is maintained in most visual areas (Sereno et al. 1995; Gardner et al. 2008; Amano et al. 2009). This might lead to the conclusion that our perception must be retinotopic, while in fact it is often *non-retinotopic*. For example, the retinal image shifts with every saccadic eye movement, but we do not perceive the world to move. In addition, when objects in the visual scene move, they fall on a new location on the retina and are consequently processed by a new set of neurons at every moment. Despite this, the world appears stable and continuous and we have no trouble perceiving moving objects.

The problem of visual stability across saccades has been studied extensively, and mechanisms ranging from no compensation (i.e., vision starts anew after each saccade) to complete compensation of the shift have been proposed (Sperry 1950; Von Holst and Mittelstaedt 1950; Duhamel et al. 1992; Bridgeman et al. 1994; Wurtz 2008; Rolfs et al. 2011). For eye movements, a key mechanism for visual stability is thought to be an efference copy of the saccadic motor command, which allows to anticipate and discount the retinal shift. In the case of object motion, the problem of stability is much more complex. Consider for example a bicycle passing by with a reflector on the spoke of its wheel. The reflector appears to move in a circular or

Published online: 30 October 2015

prolate cycloidal orbit, while in fact it traces out a curtate cycloid. We cannot see the true, absolute motion of the reflector because the motion of the bicycle is perceptually subtracted from that of the reflector (Duncker 1929; Johansson 1950), similarly to the discounting of saccadic shifts, but necessarily without the aid of efference copies. The process is automatic and unavoidable; even when knowing the true trajectory of the reflector, it remains obscure. The visual system is even able to simultaneously keep track of several reference systems moving in different trajectories, for example in a traffic situation. Despite the important role of non-retinotopic, moving reference systems in motion perception, almost nothing is known about the neural correlates.

Here, using high-density EEG, we investigate the neural encoding of non-retinotopic motion integration in the Ternus–Pikler display (Pikler 1917; Ternus 1926; Boi et al. 2009). This paradigm allows to compare motion encoding in a stationary, retinotopic reference system and a moving, non-retinotopic reference system (Fig. 1). Since the participants were instructed to fixate throughout the stimulus presentation, this study is limited to motion-based reference systems, and not aimed at dissociating between other types of non-retinotopic reference systems such as spatiotopic or craniotopic ones.

Materials and Methods

Participants

Fourteen paid students took part in the experiment. Three were excluded from further analysis due to excessive blinking and overall noisy data (>30 % rejected trials). The remaining 11 participants (seven male) were aged 21–28 years (mean 24 years). All had normal or corrected-

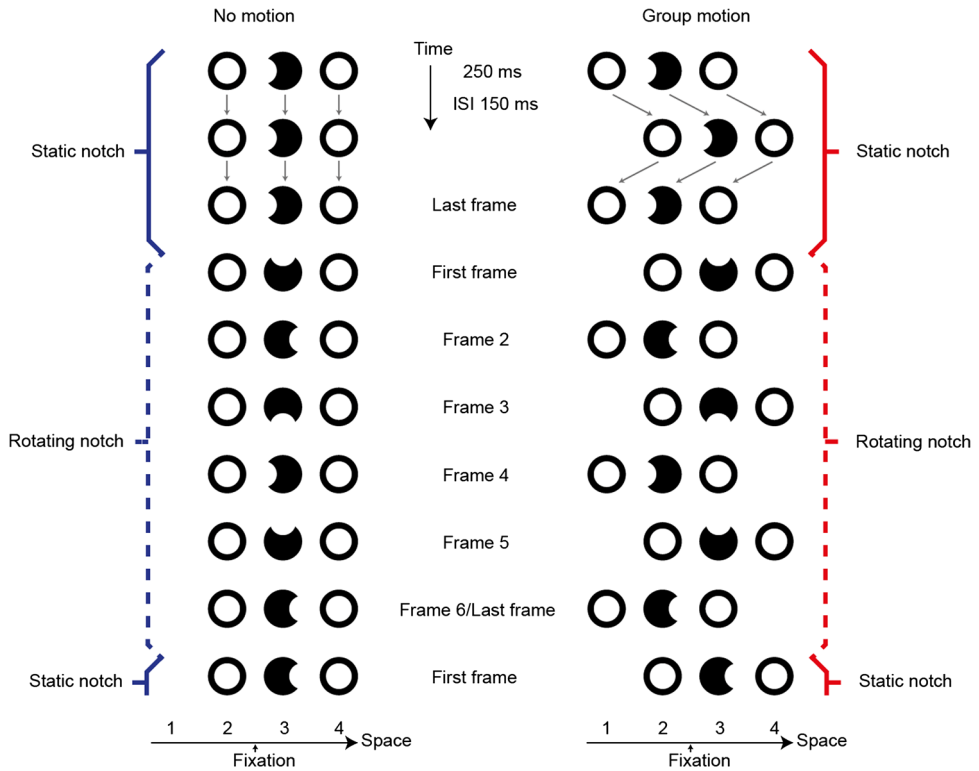

Fig. 1 Ternus-Pikler stimuli. See also Videos 1 and 2 in Supplementary material. Three disks (the *outer ones* with holes and the *central one* with a pac-man-like notch) were presented for 250 ms and followed by an inter-stimulus interval (ISI) of 150 ms. In a second frame, the disks reappeared either in the same position (No motion) or shifted one position horizontally (Group motion). After another ISI, the sequence started over again. In the No motion conditions, the disks are perceived to flicker at the same location and the notches are integrated retinotopically across frames as indicated by the *arrows* (not shown in the actual stimuli). In the Group motion conditions, the disks appear to move as a group, giving rise to a non-retinotopic reference system in which the notches in different frames are integrated across spatial locations. The notch in the *central disk* appeared either in the same position across frames (Static) or changed positions in a rotating fashion (Rotating), and transitioned between these two states at random time points. In the trials included in the EEG analysis, the notch was always rotating or static for at least six frames before the next transition. Because of randomization, all possible configurations (the three disks either in positions 1–2–3 or 2–3–4, the notch in one of the four cardinal positions) were equally likely in all frames of all conditions. The actual stimuli were *light gray* on a *dark gray* background

to-normal vision with an acuity of >0.9 in at least one eye as assessed with the Freiburg visual acuity test (Bach 1996). Ten participants reported being right-handed; one left-handed. The participants gave written informed consent before the experiment, and all procedures were in accordance with the Declaration of Helsinki and approved by the local ethics committee (protocol number 384/2011).

Stimuli and Task

In the No motion conditions, three disks were presented at the same location in a series of frames, interleaved by blank inter-stimulus intervals (ISIs; Fig. 1). In the Group motion conditions, the three disks were presented alternatingly to the left and to the right and accordingly appeared to move horizontally as a group, establishing a non-retinotopic reference system. The center disk contained a notch, which either appeared in the same position from frame to frame or shifted positions in a rotating manner. Importantly, the notch is integrated retinotopically in the No motion conditions but non-retinotopically (across space) in the Group motion conditions (see arrows in Fig. 1). In all conditions, the frame duration was 250 ms and the ISI 150 ms, which is optimal for perceiving group motion (Pantle and Picciano 1976; Breitmeyer and Ritter 1986a, b).

The participants were instructed to fixate their gaze on a red dot above the stimulus (Fig. 1), and to report the transitions from static to rotating notch as well as from rotating to static notch by pressing a hand-held push-button, emphasizing accuracy over speed. After each button-press, a sequence of 4–8 frames (in addition to the frame containing the button-press) followed before the next transition. The sequence between transitions was thus always at least five frames long. Since the sequence length was randomized, it was not possible to foresee when the next transition would occur. The notch could be in any cardinal position (up, down, left, right), and the three disks could be either to the left (positions 1–2–3 in Fig. 1) or to the right (positions 2–3–4 in Fig. 1) in the transition frame. Also the rotation direction (clockwise or counterclockwise) was randomized. Each stimulus block consisted of only No motion or only Group motion trials, and the order of the blocks was randomized. The starting position of the disks (left or right) in a block was also randomized. The disks were thus presented either to the left or to the right throughout each block of No motion trials.

If there was no button-press within 3 s after a transition, this counted as a time-out and the next transition occurred 4–8 frames after this limit. No feedback was given during the recordings. After each block of 10 trials (each transition counting as one trial) there was a 10 s pause during which a countdown of the remaining time until the next block was displayed. The last 3 s were accompanied by beeps. A recording run consisted of 6 blocks and lasted approximately 5 min. After each run, the participants were offered a short break. Ten runs were recorded per observer, resulting in a total of 600 trials. The participants used their right hand for pushing the button in half of the runs and their left hand in the other half, changing hands between each run. They were instructed to blink as little as possible during stimulus presentation, and instead blink or close their eyes during the 10 s pauses.

The stimuli were presented on a ViewSonic Graphic Series G90f+ CRT monitor controlled by a PC. The observers were seated 1.5 m from the screen in a dimly lit room (approximately 0.5 lx). The diameter of each disk was 1.5° of visual angle and the center-to-center spacing was 2.2°. The notch in the center disk was a circular shape with the same luminance as the background and a diameter of 1°, extending 0.7° into the disk. In the outer disks, there were instead circular holes of the same diameter as the notch, centered on the disks. The fixation dot was presented 0.8° above the upper edge of the stimulus, and had a diameter of 4′. The luminance of the disks and the fixation dot was 8 cd/m^2. The background as well as the notch and the holes in the disks had a luminance of 2 cd/m^2. We used these low luminance values in order to better detect motion signals in the EEG. Low luminance and contrast typically generate motion-related rather than pattern-specific evoked responses (Kuba et al. 2007). Even with these luminance levels, the participants were able to perform the task with high accuracy. A transition was considered detected if there was a button-press between 200 and 2000 ms after the onset of the First frame and no other button-presses before the next transition.

Note that because of randomization, all images were equally likely to appear in all frames of all conditions. The conditions are defined by the preceding sequence of frames rather than by the image in each frame alone, and the apparent motion percepts depend on integration across frames.

EEG Recording

The electroencephalography (EEG) recordings were carried out in an electrically shielded room. We used a Biosemi Active Two system (Biosemi, Amsterdam, the Netherlands) with 192 Ag–AgCl sintered active electrodes. The cap was placed with the Cz electrode located halfway between inion and nasion, and equally far from each ear. The recording was referenced to the CMS-DRL ground, a feedback loop that keeps the montage potential close to amplifier zero (www.biosemi.com). To detect blinks, we also recorded the electro-oculogram (EOG) with electrodes above and below the right eye as well as lateral to the left

and right outer canthus. The recording sampling rate was 2048 Hz. We later down-sampled the data off-line to 512 Hz and applied a Butterworth band-pass filter (1–40 Hz). We also used a notch filter at 50 Hz, and removed the DC drift.

EEG Data Processing

The four Ternus–Pikler conditions (Fig. 1) make up a 2-by-2 factorial design with factors Notch (Static and Rotating) and Reference system (No motion and Group motion), and both the behavioral and the EEG data were analyzed using two-way repeated measures ANOVAs with participants as random factor.

We analyzed the event-related potentials (ERPs) separately for each epoch of 400 ms. The EEG epochs start at the frame onset and comprise the duration of the frame (250 ms) as well as the ISI (150 ms). Note that in each such epoch there is no real motion but only a static image of three disks (and the ISI). Since the stimuli are periodic and a new image frame appeared every 400 ms, there is no pre-stimulus period. In the EEG analysis, we only took into account correct trials with a reaction time (RT) of at least 400 ms. The sequence between transitions was at least 6 frames long in these trials. The RT limit was set to ensure that there were no button-presses during the First frame epoch. For the RTs to reflect the EEG data, the same inclusion criteria were used for the RT analysis. Noisy epochs were excluded using a semi-automated rejection procedure with a threshold of $\pm$ 75 μV in both EEG and EOG channels. Noisy channels were excluded from this criterion for all the data of the participant in question. On average across observers, 526 (SD 42) out of 600 of the trials were included for the First frame, and 527 (SD 42) out of 600 for the Last frame. For frames 2–8, the corresponding number was 477 (SD 67) on average. We averaged the selected trials within participant and condition. No baseline correction was applied, the reasons for which are twofold. First, baseline correction would cause any "pre-stimulus" differences between the conditions to influence the post-stimulus results. Second, since the stimuli are periodic with a new image appearing every 400 ms (the duration of the EEG epoch), there is no time period suitable to use for baseline correction. We inspected the single-subject averages, and interpolated noisy channels. The average number of interpolated channels was 15 (SD 8) across observers for the First frame, and 18 (SD 9) for the Last frame. For frames 2–8, on average 18 (SD 9) electrodes were interpolated. We computed grand-averages per condition using the average reference, after normalizing individual averages subject-wise to the GFP, in order for the participants to contribute equally to the grand-averages (see explanation of GFP below).

We assessed modulations in response strength by analyzing the global field power (GFP). The GFP is the standard deviation of the electrical potentials across the scalp and gives a measure of the response strength for each time point (Lehmann and Skrandies 1980). An advantage of analyzing GFP rather than single electrode traces is that all electrodes are taken into account and the results are therefore not dependent on the choice of electrode (with the caveat that small local signals might not be as obvious). In addition, the GFP is less noisy than single-electrode traces and independent of the reference used. To account for multiple comparisons across time (the 205 time samples), we corrected the p value thresholds per effect such that the false discovery rate (FDR; Benjamini and Hochberg 1995; Genovese et al. 2002) across time samples was 5 %. We also computed the average GFP in the early, intermediate, and late latency intervals of the First frame, Last frame, and Frames 2–8. The time intervals chosen for these intervals comprised the evoked peaks in the majority of the single-subject averages. Frames 2-8 were only analyzed for exploratory reasons, and no statistical testing was applied.

The GFP summarizes all electrodes into one measure per time point. Together with the topographic information (the spatial configuration of the scalp potentials), it gives additional information and neurophysiological interpretability as compared to single-electrode analysis (Murray et al. 2008). To assess topographic differences, we first created a limited set of topographic template maps based on the grand-average data. The correlation between the maps was limited to maximum 80 %. We identified the template maps using the atomize and agglomerate hierarchical clustering (AAHC) algorithm (Murray et al. 2008). The number of template maps that best explains the data was determined by the global minimum of the cross validation (CV) value (Pascual-Marqui et al. 1995). The CV value is the ratio between the global explained variance of the AAHC result and the degrees of freedom in the model (the number of maps). Thus, the number of maps is kept as low as possible, while still keeping a good fit to the data. We then used the template maps to summarize and visualize the topographic properties of the grand-average data. The single-subject averages were compared with the template maps, and each time point was labeled with the map with the highest spatial correlation. Finally, we analyzed the single-subject occurrences of each map that displayed differences in the grand-average segmentation.

In order to estimate the current densities underlying the data, we used a local auto-regressive average (LAURA) inverse solution (Grave de Peralta Menendez et al. 2004). LAURA is a linear, distributed inverse solution that is based on biophysical constraints, and has been found to adequately locate sources of brain activity (Plomp et al. 2010). We used a solution space of 5012 evenly spread

source points within the gray matter of the Montreal Neurological Institute (MNI) 152 template brain. The lead field for the 192 electrodes was computed using a locally spherical model (LSMAC; Brunet et al. 2011). This allowed us to estimate current densities for each participant, condition, and time point. The analysis was restricted to the time average of the current densities in periods where we had found GFP differences between the conditions. We tested each source point separately and used FDR correction of the p value thresholds per effect across source points. The locations of the source points are reported in Talairach coordinates (Talairach and Tournoux 1988).

For comparison with single-electrode studies, we also performed a single-electrode analysis. All time samples of all electrodes (average referenced) were tested, and the FDR was limited to 5 % across all tests (electrodes and time samples).

The EEG data analysis was performed using the Cartool software by Denis Brunet (https://sites.google.com/site/fbmlab/cartool). We used the statistical language R (http://www.r-project.org/) for the statistical analysis.

In addition to the analysis described above, we also performed a Bayesian analysis on the GFP traces using the BayesFactor package described in Rouder et al. (2012).

Results

Behavior

The participants fixated on a dot above the stimuli. To ensure attention to the stimuli, they were asked to indicate the transitions between notch states by pushing a button, emphasizing accuracy over speed. Transitions to rotating notches were more often detected than transitions to static notches (main effect of Notch: $F(1,10) = 32.9$, $p < 0.0001$; No motion/Static 83 % ± 7 (mean ± SD), No motion/Rotating 94 % ± 6, Group motion/Static 83 % ± 7, Group motion/Rotating 95 % ± 7). There was no significant difference in performance between the No motion and the Group motion conditions (main effect of Reference system, $p = 0.81$) and no interaction effect ($p = 0.73$). In total for all conditions, there were only 1.3 ± 1.3 false positive responses per participant. The high performance indicates that the participants were attending to the notch, and that they could detect the transitions in both the No motion and the Group motion reference systems without difficulty. These results also confirm that the stimuli are integrated retinotopically in the No motion conditions and non-retinotopically in the Group motion conditions as described in Fig. 1 and previously found in psychophysical studies (Pantle and Picciano 1976; Boi et al. 2009).

Only correct trials with a reaction time of at least 400 ms (the duration of the EEG epoch) were included in the EEG and reaction time (RT) analyses. We found no significant RT differences (main effect of Notch: $p = 0.50$, main effect of Reference system: $p = 0.11$, interaction effect: $p = 0.61$; No motion/Static 653 ms ± 85, No motion/Rotating 650 ms ± 157, Group motion/Static 692 ms ± 87, Group motion/Rotating 670 ms ± 163).

EEG: Global Field Power

We first investigated the differences between the retinotopic and the non-retinotopic reference systems (No motion vs. Group motion) by analyzing the response strength as measured by the GFP (Lehmann and Skrandies 1980). We analyzed the First and the Last frame separately (see Fig. 1). The First frame constitutes the transition between notch states (from rotating to static, or from static to rotating), while the Last frame represents an established perceptual state. We expected relatively large differences between the two reference systems because of the salient horizontal motion in the Group motion conditions, which is absent in the No motion conditions. Surprisingly, we found no statistically significant main effect of Reference system or interaction effect in either the First or the Last frame (Fig. 2a, b). In fact, the GFP traces are overall similar in both reference systems in both the First and the Last frame: the GFP traces of the Static notch conditions (solid lines) follow each other throughout the epochs, and the same holds for the Rotating notch conditions (dashed lines). The largest deviation from this is found around 200–250 ms after stimulus onset in the First frame, where the GFP is higher in the No motion/Rotating condition than the Group motion/Rotating one (Fig. 2a). Although this effect is as mentioned not significant, it might reflect a differential encoding of the notch rotation in the two reference systems. However, it does not signify a general difference between the reference systems, since it is visible only between the Rotating notch conditions, and only in a limited period of the First frame. Thus, despite the horizontal motion of the entire stimulus in the Group motion conditions, we found no significant differences between the two reference systems.

Second, we found large differences between the Rotating and Static notch conditions in both the First and the Last frame. In addition, these differences are similar in both reference systems: As mentioned, the GFP traces of the No motion/Static and Group motion/Static conditions are similar, and the same holds true for the No motion/Rotating and Group motion/Rotating conditions (main effect of Notch, Fig. 2a, b). Thus, it seems that even though the notch is integrated retinotopically in the No motion reference system but non-retinotopically in the Group motion one, it is encoded similarly in both reference systems.

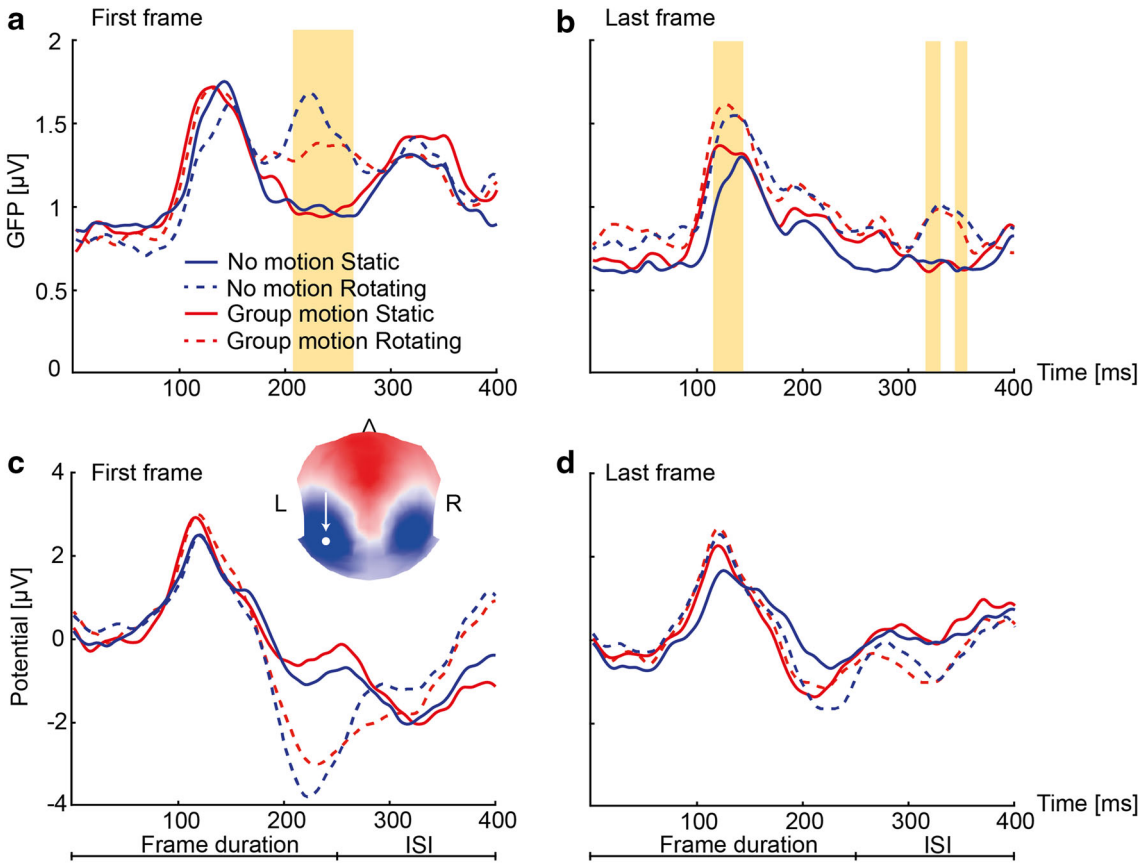

Fig. 2 Global field power (GFP) and single-electrode event-related potentials (ERPs). Periods of significantly higher GFP for Rotating than Static notches are marked by *yellow bars* (FDR 5 % across time samples, per effect). **a** First frame. The GFP is higher in the Rotating than in the Static notch conditions in an intermediate latency interval (207–264 ms). Importantly, there is no significant main effect of Reference system and no interaction effect. Note that since the stimuli are periodic, there is no "pre-stimulus period". **b** Last frame. The GFP is higher for Rotating than Static notches in an early (115–143 ms) and in two late intervals (316–330 ms and 344–355 ms). Again, there are no other effects. **c** Single-electrode ERPs from a posterior electrode (E30) in the epicenter of the peak in the intermediate interval of the First frame (*white arrow* marked on the average No motion/Rotating topography in this interval) are shown for comparison. These traces resemble the GFP ones, except that both negative and positive potentials are reflected in positive GFP. *Color-coding* is as in **a**

Third, we compared the First and the Last frame results. In the First frame, the GFP is higher in the Rotating than in the Static conditions in both reference systems at an intermediate latency (main effect of Notch at 207–264 ms, Fig. 2a). The stronger response in the Rotating conditions resembles a typical motion onset N2 component (Kuba et al. 2007). Importantly, the rotation-related activity is not simply due to the rotation per se, since it is only present in the First frame, while the notch continues to rotate until the Last frame. Neither is it related to target detection or response preparation, since it is absent in the Static notch conditions which are also targets. The N2 component is usually found 160–200 ms after stimulus onset, i.e., earlier than in our data. However, its latency has been shown to vary depending on for example contrast level (Kubová et al. 1995) and the type of apparent motion (Tanaka et al. 2007). In the Last Frame, the GFP traces overall look different compared to the First frame: The motion onset component at 207–264 ms is absent, and instead the GFP is significantly higher in the Rotating than in the Static conditions in an early (115–143 ms) and two late intervals (316–330 ms and 344–355 ms; Fig. 2b).

To investigate how the neural encoding of the notch in the novel state (First frame) evolves to the established state (Last frame), we computed the GFP in Frames 2–8, in addition to the First and Last frames. If the intermediate latency effect in the First frame (higher GFP for Rotating than Static notches at 207–264 ms) is related to the onset of rotation, as we suggest, it should diminish in the following frames. Indeed, the effect is specific for the First frame and quickly subsides in the following frames (Fig. 3). From Fig. 3 it is also obvious that the GFP amplitudes are larger in the First frame compared to all other frames in both the early and the late component, possibly owing to target

detection or response preparation. Further, the differences between Rotating and Static notches in the early (~130 ms) and late (~340 ms) intervals found in the Last frame are visible already from Frame 3 on. This higher GFP for Rotating than Static notches might be due to a higher attentional state in the more salient Rotating notch conditions. Specifically, the early component resembles a P1 response, which is known to depend on attention level and has been shown to increase both with spatial and non-spatial attention (Taylor 2002; Nobre et al. 2006; Klimesch 2011). The results from Frames 2–8 should be interpreted with care since they might be influenced by button-presses (Frames 2–5) and include fewer trials (particularly from Frame 7 onwards since the minimum sequence length was 6 frames). Nevertheless, these data indicate that the First frame GFP traces have distinct appearances compared to the other frames.

EEG: Topographic Analysis and Inverse Solutions

Up to now, we have focused on the GFP, which collapses the 192 electrode traces into one measure per time point. To localize the active brain regions, we first analyzed the distributions of voltages across the scalp (topographies). Topographic differences between conditions indicate differences in the underlying brain activations, which can then be estimated using inverse solutions. In the First frame epoch, we targeted the intermediate period (~230 ms) where we had found significantly higher GFP in the Rotating than in the Static conditions. We found a distinct topographic map that is more expressed in the Rotating than in the Static conditions (Fig. 4a) and two other maps that are instead more expressed in the Static conditions (Supplementary Fig. 1). The rotation topography has a posterior negative deflection which is absent in the Static conditions and typically found in the N2 component associated with the onset of both real and apparent motion (Kuba et al. 2007). In the Last frame, we targeted the early (~130 ms) and the late (~340 ms) intervals where, again, we had found significantly higher GFP in the Rotating than in the Static notch conditions. In the early interval, the topographies are similar in all conditions (Supplementary Fig. 1). In the late interval, one topographic map is more present in the Rotating conditions (Fig. 4c) while two other maps are instead more expressed in the Static conditions (Supplementary Fig. 1).

As mentioned, topographic differences indicate differences in brain activation. To identify these differences, we estimated the current densities underlying the EEG using a distributed inverse solution (LAURA; Grave de Peralta Menendez et al. 2004). In the intermediate period (~230 ms) of the First frame, where we had found highest GFP and in addition a distinct topography in the Rotating conditions, the estimated main source of the rotation activity is in the right middle temporal gyrus (main effect of Notch, FDR 10 %, Talairach coordinates of most significant voxel: 42, −59, 18; Fig. 4b). This is close to the human motion processing complex (hMT+), which is known to be involved in the processing of both real and apparent motion (Goebel et al. 1998; Muckli et al. 2002; Liu et al. 2004). We report the results at 10 % FDR, since at 5 % FDR no voxels survived thresholding, and the purpose here was to identify the most likely source of the significant topographic differences. In the early interval (~130 ms) of the Last frame, we found no significant current density differences, as expected considering the similar topographies in all conditions. In the late interval (~340 ms) of the Last frame, where we had found highest GFP and a distinct topography in the Rotating conditions, current densities are higher in the Rotating than in the

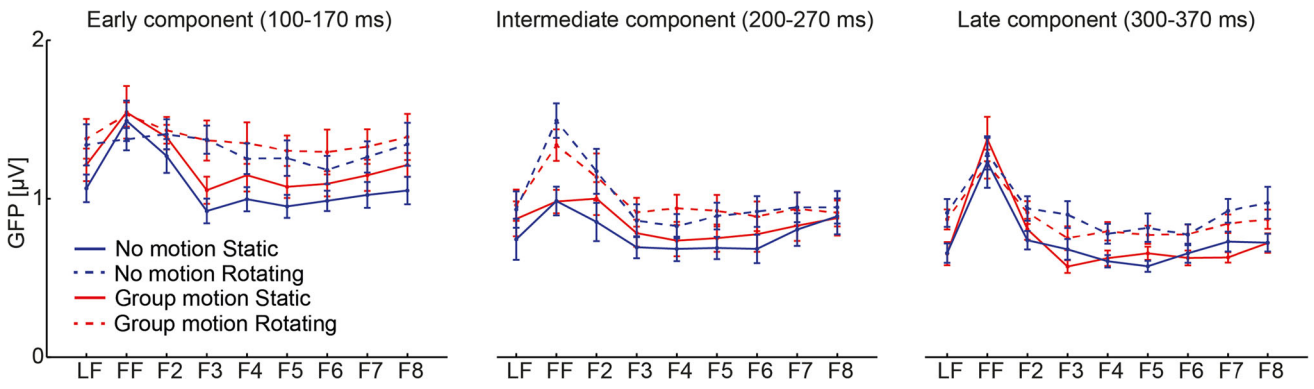

Fig. 3 GFP for the Early (100–170 ms), Intermediate (200–270 ms) and Late (300–370 ms) latency components for all four conditions in the Last frame (*LF*), First frame (*FF*), and Frames 2-8 (*F2-F8*). The First frame displays the highest GFP in all three intervals compared to the other frames, indicating more neural processing for novel notch states. In addition, the GFP is higher overall for the Rotating (*dashed lines*) than for the Static conditions (*solid lines*). In the Intermediate component, this effect is most pronounced for the First frame. Note that Frames *6-8* contain some trials that also contribute to the Last frame data. No statistical analysis was performed. *Bars* are ±1 SEM

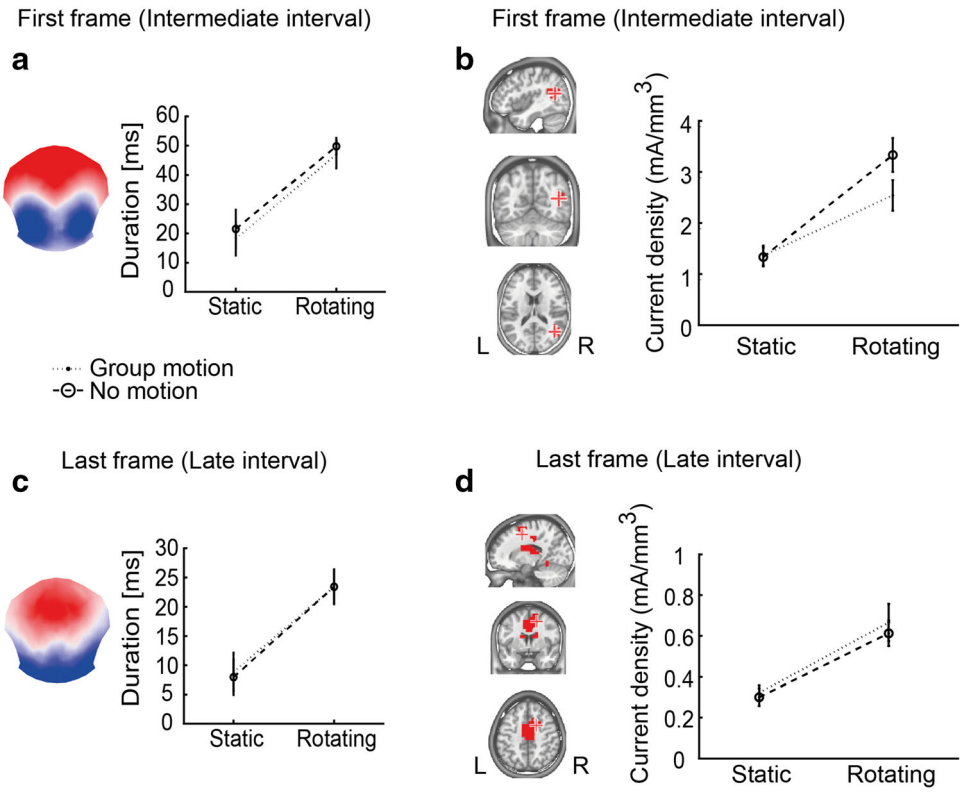

Fig. 4 Topographic and source analyses. **a** First frame, intermediate interval (207–264 ms). A distinct rotation topography is expressed ~30 ms longer in the Rotating than in the Static conditions (main effect of Notch: $F(1,10) = 51.3$, $p < 0.0001$). There are no other significant effects for this topographic map (main effect of Reference system: $p = 0.44$, interaction effect: $p = 0.95$). *Blue* indicates negative and *red* indicates positive potentials. **b** Using source analysis, we estimated the brain activity underlying the time-average EEG in the same interval as in **a**. No voxels survived thresholding at 5 % FDR. Voxels showing higher current density in the Rotating than the Static conditions at 10 % FDR are shown in *red* in sagittal, coronal, and transverse views. The most significant voxel is in the right middle temporal gyrus and is marked by a cross. In this voxel, the current density is about twice as high for Rotating compared to Static notches (*rightmost graph*). There are no other effects at this significance level. Condition coding is as in **a**. **c** Last frame, late interval (316–330 ms and 344–355 ms collapsed). Also in this interval, the Rotating conditions display a distinct topography ($F(1,10) = 38.7$, $p < 0.0001$). There are no other significant effects for this topography (main effect of Reference system: $p = 0.86$, interaction effect: $p = 0.86$). **d** The estimated source of the activity in the Rotating conditions averaged over the same interval as in **c** is in an area centered in the right cingulate gyrus (FDR 5 %). Again, the most significant voxel displays about twice as high current density in the Rotating compared to the Static conditions. There are no other effects at this significance level. *Bars* are ±1 SEM

Static conditions in a region centered on the right cingulate gyrus in the limbic lobe, extending into the frontal lobe and thalamus (main effect of Notch, FDR 5 %, Talairach coordinates of most significant voxel: 16, 5, 45; Fig. 4d). This area has been identified as part of an extensive attention network (Mesulam 1981; Posner and Petersen 1990).

For one of the four topographic maps in the late period of the Last frame, we found a small main effect of Reference system and a small interaction effect (Supplementary Fig. 1). Apart from this, there are no main effects of Reference system or interaction effects in either the GFP, topographic or source analyses, in either the First or Last frame.

Supplementary Analyses

For comparison with single-electrode studies, we performed a single-electrode analysis where the EEG amplitudes of all time samples of all electrodes were tested. In agreement with our results so far, we found strong differences between Static and Rotating notches (main effects of Notch, Supplementary Fig. 2a, b) and only minor differences between the No motion and Group motion reference systems (main effect of Reference system, Supplementary Fig. 2c, d) and interaction effects (Supplementary Fig. 2e, f). Supplementary Fig. 3 shows butterfly plots of the grand-average single-electrode traces of all conditions.

In order to shed further light on the influence of each of the effects in the ANOVA design, we performed a supplementary Bayesian analysis of the GFP traces (Supplementary Fig. 4). As in the standard analysis, the main effects of Notch dominate throughout most of the visual processing, and there are no significant interaction effects. However, we also found a clear early effect of Reference system around 100–120 ms after frame onset in both the First and the Last frame.

Discussion

We used high-density EEG to investigate the neural correlates of relative motion encoding in the Ternus–Pikler display. While we were able to pick up strong signals related to the small target notch in the central disk, the large motion of the entire display was hardly visible in the EEG response. The inverse solutions indicate that the stronger activations in the Rotating conditions might stem from extrastriate areas, including the right temporal gyrus and the right cingulate gyrus. While the absence of significant differences between the two reference systems (No motion and Group motion) does not necessarily mean that the encoding is the same in both, it is interesting to note these null results in combination with the large main effects of Notch. A supplementary Bayesian analysis of the GFP traces did reveal an early effect of Reference system 100–120 ms after frame onset, after which the main effects of Notch dominate. This could be interpreted as an early encoding of the Reference system, which is then discounted in favor of a similar encoding of the notch state (static or rotating) in both Reference systems. This reference system independent encoding of the notch is visible throughout the rest of the visual processing.

It is important to note that the different EEG responses in the different conditions are not due to motion presented during the EEG epochs, since in each epoch of 400 ms there is no motion but only a static image of three disks and the ISI. Moreover, the results cannot be explained by differences in the static images since all eight images appeared in all frames of all conditions equally often (Fig. 1). Eye movements are not likely to have caused the results, since participants were instructed to fixate throughout the stimulus presentation, and observers have been shown to fixate well in similar Ternus–Pikler paradigms even without fixation dot (Boi et al. 2009). Hence, the differences are likely due to the specific integration of information across image frames in each condition, and the resulting percepts.

To perceive the notch relative to the reference system of the three disks, the motion of the disks first has to be computed. We were therefore surprised to find such strong correlates of the encoding of the notch compared to the encoding of the reference system. Clearly, the motion of the reference system has to be encoded at some stage of the visual processing. Our results suggest that this is done around 100–120 ms after stimulus onset, allowing a largely reference system independent encoding of the motion of the notch throughout the rest of the visual processing. In the example of the bicycle, this would mean that the reflector motion is encoded similarly throughout most of the visual processing regardless of whether the bicycle is moving forward or the wheel is simply spun in the air.

To our knowledge, this is the first electrophysiological study directly investigating the encoding of motion relative to a moving reference system. Several previous studies have investigated the encoding of biological motion, which often relies on relative motion encoding. In many of these studies, the superior temporal sulcus (STS) has been pointed out as the key region (reviewed in Allison et al. 2000; Decety and Grèzes 1999). However, these findings are specific to biological motion and not applicable to relative motion encoding in general.

Acknowledgments We thank Marc Repnow for technical support. This work was supported by the Swiss National Science Foundation (SNF) Project "Basics of visual processing: from retinotopic encoding to non-retinotopic representations".

References

Allison T, Puce A, McCarthy G (2000) Social perception from visual cues: role of the STS region. Trends Cogn Sci 4:267–278

Amano K, Wandell BA, Dumoulin SO (2009) Visual field maps, population receptive field sizes, and visual field coverage in the human MT+ complex. J Neurophysiol 102:2704–2718. doi:10.1152/jn.00102.2009

Bach M (1996) The "Freiburg Visual Acuity Test"—automatic measurement of the visual acuity. Optom Vis Sci 73:49–53

Benjamini Y, Hochberg Y (1995) Controlling the false discovery rate: a practical and powerful approach to multiple testing. R Stat Soc Ser B 57:289–300

Boi M, Ögmen H, Krummenacher J et al (2009) A (fascinating) litmus test for human retino- vs. non-retinotopic processing. J Vis 9:1–11. doi:10.1167/9.13.5

Breitmeyer BG, Ritter A (1986a) The role of visual pattern persistence in bistable stroboscopic motion. Vis Res 26:1801–1806

Breitmeyer BG, Ritter A (1986b) Visual persistence and the effect of eccentric viewing, element size, and frame duration on bistable stroboscopic motion percepts. Percept Psychophys 39:275–280

Bridgeman B, Van der Heijden AHC, Velichkovsky BM (1994) A theory of visual stability across saccadic eye movements. Behav Brain Sci 17:247–258. doi:10.1017/S0140525X00034361

Brunet D, Murray MM, Michel CM (2011) Spatiotemporal analysis of multichannel EEG: CARTOOL. Comput Intell Neurosci 2011:813870. doi:10.1155/2011/813870

de Peralta Grave, Menendez R, Murray MM, Michel CM et al (2004) Electrical neuroimaging based on biophysical constraints. Neuroimage 21:527–539. doi:10.1016/j.neuroimage.2003.09.051

Decety J, Grèzes J (1999) Neural mechanisms subserving the perception of human actions. Trends Cogn Sci 3:172–178

Duhamel J-R, Colby CL, Goldberg ME (1992) The updating of the representation of visual space in parietal cortex by intended eye movements. Science 255:90–92

Duncker K (1929) Über induzierte Bewegung. (Eine Betrag zur Theorie optisch wahrgenommener Bewegung.). Psychol Forsch 12:180–259

Gardner JL, Merriam EP, Movshon JA, Heeger DJ (2008) Maps of visual space in human occipital cortex are retinotopic, not spatiotopic. J Neurosci 28:3988–3999. doi:10.1523/JNEUROSCI.5476-07.2008

Genovese CR, Lazar NA, Nichols T (2002) Thresholding of statistical maps in functional neuroimaging using the false discovery rate. Neuroimage 15:870–878. doi:10.1006/nimg.2001.1037

Goebel R, Khorram-Sefat D, Muckli L et al (1998) The constructive nature of vision: direct evidence from functional magnetic resonance imaging studies of apparent motion and motion imagery. Eur J Neurosci 10:1563–1573

Johansson G (1950) Configurations in event perception, an experimental study. Almqvist & Wiksells, Uppsala

Klimesch W (2011) Evoked alpha and early access to the knowledge system: the P1 inhibition timing hypothesis. Brain Res 1408:52–71. doi:10.1016/j.brainres.2011.06.003

Kuba M, Kubová Z, Kremlácek J, Langrová J (2007) Motion-onset VEPs: characteristics, methods, and diagnostic use. Vis Res 47:189–202. doi:10.1016/j.visres.2006.09.020

Kubová Z, Kuba M, Spekreijse H, Blakemore C (1995) Contrast dependence of motion-onset and pattern-reversal evoked potentials. Vis Res 35:197–205

Lehmann D, Skrandies W (1980) Reference-free identification of components of checkerboard-evoked multichannel potential fields. Electroencephalogr Clin Neurophysiol 48:609–621

Liu T, Slotnick SD, Yantis S (2004) Human MT+ mediates perceptual filling-in during apparent motion. Neuroimage 21:1772–1780. doi:10.1016/j.neuroimage.2003.12.025

Mesulam MM (1981) A cortical network for directed attention and unilateral neglect. Ann Neurol 10:309–325

Muckli L, Kriegeskorte N, Lanfermann H et al (2002) Apparent motion: event-related functional magnetic resonance imaging of perceptual switches and States. J Neurosci 22:RC219

Murray MM, Brunet D, Michel CM (2008) Topographic ERP analyses: a step-by-step tutorial review. Brain Topogr 20:249–264. doi:10.1007/s10548-008-0054-5

Nobre AC, Rao A, Chelazzi L (2006) Selective attention to specific features within objects: behavioral and electrophysiological evidence. J Cogn Neurosci 18:539–561. doi:10.1162/jocn.2006.18.4.539

Pantle A, Picciano L (1976) A multistable movement display: evidence for two separate motion systems in human vision. Science 193:500–502

Pascual-Marqui RD, Michel CM, Lehmann D (1995) Segmentation of brain electrical activity into microstates: model estimation and validation. IEEE Trans Biomed Eng 42:658–665. doi:10.1109/10.391164

Pikler J (1917) Sinnesphysiologische Untersuchungen. Barth, Leipzig

Plomp G, Michel CM, Herzog MH (2010) Electrical source dynamics in three functional localizer paradigms. Neuroimage 53:257–267. doi:10.1016/j.neuroimage.2010.06.037

Posner MI, Petersen SE (1990) The attention system of the human brain. Annu Rev Neurosci 13:25–42. doi:10.1146/annurev.ne.13.030190.000325

Rolfs M, Jonikaitis D, Deubel H, Cavanagh P (2011) Predictive remapping of attention across eye movements. Nat Neurosci 14:252–256. doi:10.1038/nn.2711

Rouder JN, Morey RD, Speckman PL, Province JM (2012) Default Bayes factors for ANOVA designs. J Math Psychol 56:356–374

Sereno MI, Dale AM, Reppas JB et al (1995) Borders of multiple visual areas in humans revealed by functional magnetic resonance imaging. Science 268:889–893

Sperry RW (1950) Neural basis of the spontaneous optokinetic response produced by visual inversion. J Comp Physiol Psychol 43:482–489

Talairach J, Tournoux P (1988) Co-planar stereotaxic atlas of the human brain: 3-D proportional system: an approach to cerebral imaging. Thieme, New York

Tanaka E, Noguchi Y, Kakigi R, Kaneoke Y (2007) Human cortical response to various apparent motions: a magnetoencephalographic study. Neurosci Res 59:172–182. doi:10.1016/j.neures.2007.06.1471

Taylor MJ (2002) Non-spatial attentional effects on P1. Clin Neurophysiol 113:1903–1908

Ternus J (1926) Experimentelle Untersuchung über phänomenale Identität. Psychol Forsch 7:81–136

Von Holst E, Mittelstaedt H (1950) Das Reafferenzprinzip. (Wechselwirkungen zwischen Zentralnervensystem und Peripherie). Naturwissenschaften 37:464–476

Wurtz RH (2008) Neuronal mechanisms of visual stability. Vision Res 48:2070–2089. doi:10.1016/j.visres.2008.03.021